

## Polarization observations of lightning-produced VHF emissions by the FORTE satellite

Xuan-Min Shao and Abram R. Jacobson

Space and Atmospheric Sciences Group, Los Alamos National Laboratory, Los Alamos, New Mexico, USA

Received 2 July 2001; revised 25 January 2002; accepted 4 February 2002; published 23 October 2002.

[1] Following an earlier polarization study for a well-defined man-made very high frequency (VHF) signal by using the two orthogonally oriented, linear polarization antennas aboard the FORTE satellite, we report in this paper similar polarization observations for lightning-produced radiation. A selected group of 313 transionospheric pulse pairs (TIPPs) that were geolocated by the National Lightning Detection Network (NLDN) has been analyzed. The TIPPs have been examined with high time resolution so that the magnetoionic modes can be resolved. Most of the TIPPs have been found highly polarized, with 40% of them far above the background polarization level. The polarization ellipticity and the orientation of the ellipse of the split modes have been examined as a function of the nadir and the azimuthal angles as referenced to satellite coordinates, and they are found in agreement with the predictions based on the antenna beam pattern. The original and the reflected pulses in a TIPP show nearly the same properties of polarization, except the latter appears less polarized. However, no recognizable polarization has been observed for the VHF signals accompanying more common discharge processes of initial ground strokes, dart leaders, and K streamers that usually produce continuous VHF radiation. Observations of a sequence of impulsive radiation bursts that is apparently associated with a normal negative cloud-to-ground flash indicate they are somewhat polarized, though not as much as the TIPPs. On the basis of the polarization observations, the possible breakdown mechanisms that are responsible for the VHF radiation have been discussed. For the highly polarized TIPP events, if they follow a cone-shaped discharge geometry, the half-angle of the cone is estimated to be less than  $22^\circ$ .

*INDEX TERMS:* 3324 Meteorology and Atmospheric Dynamics: Lightning; 3394 Meteorology and Atmospheric Dynamics: Instruments and techniques; 6964 Radio Science: Radio wave propagation; 2494 Ionosphere: Instruments and techniques; *KEYWORDS:* Lightning, lightning electromagnetic radiation, polarization, ionospheric propagation

**Citation:** Shao, X.-M., and A. R. Jacobson, Polarization observations of lightning-produced VHF emissions by the FORTE satellite, *J. Geophys. Res.*, 107(D20), 4430, doi:10.1029/2001JD001018, 2002.

### 1. Introduction

[2] In a previous paper [Shao and Jacobson, 2001] we described in detail the principles and techniques used for polarization studies of broadband VHF signals via the FORTE (Fast On-Orbit Recording of Transient Events) satellite observations. The FORTE satellite was launched on 29 August 1997 into a  $70^\circ$  inclination, nearly circular orbit at 800 km altitude. The satellite carries two linearly polarized, log-periodic dipole array antennas (LPA) that are orthogonal to each other along the same boom pointing toward the satellite's nadir. Each antenna can be fed into a separate broadband (25 MHz Nyquist bandwidth) radio receiver, and the two receivers can be set up to take data coherently with the two receivers phase-synchronized to a

common reference signal. This type of antenna-receiver setup allows us to thoroughly examine the polarization properties for received radio signals. In the paper by Shao and Jacobson [2001], analyses focused on the powerful, linearly polarized impulsive VHF signals generated by the Los Alamos Portable Pulser (LAPP). With this type of well-defined signal, the effects of the Earth's ionosphere and magnetic field on the VHF radio propagation and polarization were investigated. The framework concerning effects of the FORTE antenna beam pattern over the polarization measurements was established and tested. One case of TIPP [Holden *et al.*, 1995] produced by a lightning discharge was analyzed and represented for its polarization properties.

[3] In this paper we will broaden our polarization investigations for lightning-produced VHF signals by using essentially the same techniques laid out in the previous paper. Polarization observations of VHF signals produced by lightning discharges have not been conducted or reported

elsewhere. Such observations on the ground are difficult to conduct since the conducting Earth and the surrounding structures near the observation site could substantially complicate the measurements. Without these environmental constraints, the FORTE satellite provides an ideal platform for the polarization studies. FORTE has recorded millions of lightning-produced VHF signals, and much of the data was recorded coherently by the two LPA antennas and is suitable for polarization studies.

[4] Polarization observations of the lightning-produced VHF signals offer an entirely different, new approach for looking into the physics behind the associated discharge breakdown processes. For instance, if a signal is detected purely polarized, the associated charge acceleration (current variation) that is responsible for the radiation can be inferred to be aligned along a one-dimensional linear path. If, at the other extreme, the signal is totally unpolarized (or incoherent), the corresponding processes can be inferred as being multiple and randomly oriented. In this paper, we report the polarization analysis for some selected TIPP events, as well as for other types of lightning discharges that are more commonly observed from the ground. The possible implications of the polarization observations on the corresponding breakdown processes will be discussed.

## 2. Measurement and Analysis

[5] The FORTE LPA antennas can operate at their primary frequencies of 30–90 MHz, and can also operate at their ‘high band’ mode of 90–270 MHz. For polarization measurement, the radio receivers onboard the FORTE satellite can be tuned anywhere from 20 to 300 MHz with an analog bandwidth of 22 MHz. Each analog signal is then digitized continuously by a 12-bit digitizer at the rate of 50 mega-samples per second (25 MHz Nyquist bandwidth). In this paper, we will focus only on the observations at the 26–48 MHz band (‘low band’), the same as that reported in the earlier paper [Shao and Jacobson, 2001].

[6] As described in detail by Kraus [1986] and Shao and Jacobson [2001], for a general, partially polarized plane electromagnetic wave, the four measurable Stokes parameters that describe the state of the polarization can be expressed as

$$\begin{aligned} I &= \langle E_1^2 \rangle + \langle E_2^2 \rangle = P_0 \\ Q &= \langle E_1^2 \rangle - \langle E_2^2 \rangle = P_0 \langle \cos 2\varepsilon \cos 2\tau \rangle \\ U &= 2\langle E_1 E_2 \cos(\delta_x - \delta_y) \rangle = P_0 \langle \cos 2\varepsilon \sin 2\tau \rangle \\ V &= 2\langle E_1 E_2 \sin(\delta_x - \delta_y) \rangle = P_0 \langle \sin 2\varepsilon \rangle \end{aligned} \quad (1)$$

As shown in Figure 1,  $E_1$  and  $E_2$  are the amplitudes of the electric field in the  $x$  and  $y$  directions;  $\delta_x - \delta_y$  is the phase difference between the  $x$  and  $y$  components;  $\varepsilon$  denotes the ellipticity in terms of an opening angle formed by the minor and major axes of the polarization ellipse, and the sense of the E-vector rotation by its sign ( $-45^\circ \leq \varepsilon \leq +45^\circ$ );  $\tau$  represents the tilt of the major axis relative to the  $x$  direction ( $-90^\circ \leq \tau \leq +90^\circ$ ); and  $\langle \dots \rangle$  indicates the macroscopic time average. For an ideal monotonic wave,  $E_1$ ,  $E_2$  and  $\delta_x -$

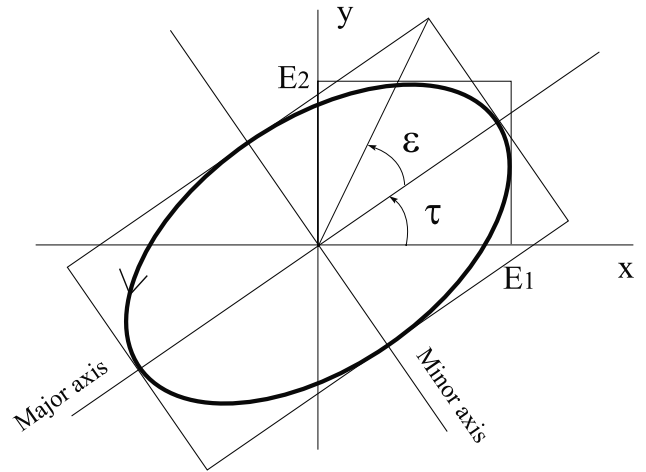


**Figure 1.** Geometry of polarization ellipse that illustrates relations of  $E_1$ ,  $E_2$  and  $\tau$ ,  $\varepsilon$ .

$\delta_y$ , are constants and will not change with time, and the wave is defined as a completely polarized wave. In such a case, the four Stokes parameters are not independent with each other, but will satisfy the relation of  $I^2 = Q^2 + U^2 + V^2$ , i.e., the total signal power equals the polarized power. In reality,  $E_1$ ,  $E_2$  and  $\delta_x - \delta_y$ , will vary with time, and the polarized power will be less than the total power. In this case the wave is considered partially polarized. In equation 1,  $I$  and  $Q$  can be regarded as the sum and difference of two autocorrelation functions of  $E_1(t)$  and  $E_2(t)$ , while  $U$  and  $V$  as the corresponding cross-correlation functions for the real and imaginary parts. The ratio

$$d = \frac{\sqrt{Q^2 + U^2 + V^2}}{I} \quad (2)$$

of the polarized power over the total power indicates the degree of polarization, which can vary in the range of 0 to 1 for completely unpolarized (or, in other words, randomly polarized) to completely polarized waves, respectively. From the degree of polarization  $d$  and the Stokes parameters,  $\varepsilon$  and  $\tau$  can be computed for the polarized portion of the wave. As being illustrated in Figure 1, for linear and circular polarizations  $|\varepsilon|$  equals to  $0^\circ$  and  $45^\circ$ , respectively, and for elliptical polarization  $|\varepsilon|$  has a value in between. The sign of  $\varepsilon$  indicates whether the E-vector rotates clockwise or anticlockwise.

## 3. Observations of TIPP Events

[7] TIPP events were first reported by Holden *et al.* [1995] from broadband VHF radio observations aboard the ALEXIS satellite. They showed that nearly every trigger of the radio system was characterized by a pair of impulsive, broadband pulses. The pulses within a pair were usually a few microseconds in duration and were typically separated by a few tens of microseconds. The VHF radiation power of the pulses was typically at least ten times greater than that produced by normal lightning discharges. Further analysis of the ALEXIS observations by Massey and Holden [1995] and Massey *et al.* [1998a] suggested that the TIPP events

were associated with thunderstorm activities, and that the second pulse of the pair was a reflection of the first off the Earth surface. With the more sophisticated radio receivers aboard the FORTE satellite, millions of TIPP-like events have been observed, not only the VHF intense ones as detected by the ALEXIS satellite but also much weaker TIPPs that are apparently associated with more familiar lightning discharges [Jacobson *et al.*, 1999]. After careful statistical analysis of the pulse separation and the corresponding line-of-sight-integrated total electron content (TEC), along which the signals propagated from the near Earth surface to the satellite, Jacobson *et al.* [1999] concluded that the second pulse of a TIPP event was indeed the reflection of the first. Ground-based electric field observations [Smith *et al.*, 1998] suggested that the brightest TIPP events observed by the ALEXIS and FORTE satellites were associated with a distinct class of in-cloud discharges that produced very large amplitude, narrow bipolar field change (LF/VLF) pulses.

[8] The FORTE lightning data has been archived with some key parameters for each triggered record. As described in detail by Jacobson *et al.* [1999], each record was first prewhitened (to suppress the narrowband carriers) and dechirped (to correct for the ionospheric dispersion), and then the power waveform is computed to recover the waveform as though there had been no effects from the carriers and the ionosphere. From the prewhitened, dechirped power waveforms, the effective pulse width ( $1/e$  half width of the first peak of the power-curve autocorrelation, see Jacobson *et al.* [1999, Figure 1]), second-pulse signal-to-noise (SNR) ratio, power “contrast” (peak to median power), and several other parameters were estimated and archived.

[9] In this paper, we will focus the polarization analysis on the geolocated, VHF-bright TIPP events. The TIPP events are first selected from the archived FORTE database for those that have a “contrast” over 50, a second-pulse SNR over 30, and a power  $1/e$  width of less than 10  $\mu\text{s}$ , for the cases in which the data was taken coherently between the two antenna-receivers at the frequency band of 26–48 MHz. The selection is then further narrowed to those that were simultaneously located by the National Lightning Detection Network (NLDN) [Cummins *et al.*, 1998] over the contiguous United States. NLDN is a ground-based array of sensors that detects low frequency (LF) and very low frequency (VLF) radiation due to vertical current of lightning discharges, predominantly ground strokes in cloud-to-ground (CG) discharges. During the periods of April–September in 1998 and May–October in 1999, we conducted cooperative observations between FORTE (VHF) and NLDN (LF/VLF) over the contiguous United States. The NLDN data were specially postprocessed in a relaxed-criterion mode to provide enhanced detection for intracloud (IC) discharges (such as the TIPP events), as well as for distant CG discharges. For the purpose of this campaign, each NLDN event was labeled “C” for IC discharge, or “G” for CG discharge. For a CG discharge the polarity and peak current are also provided. The selected FORTE TIPP events are all associated with NLDN “C” discharges. Detailed descriptions of the cooperative campaigns were reported by Jacobson *et al.*, [2000], and will not be reiterated here. Through these selection procedures,

we found 313 VHF-intense FORTE TIPPs that were geolocated by NLDN.

### 3.1. A TIPP Case Study

[10] Figure 2 shows a detailed analysis for a TIPP event that occurred at 18:14:37 UT on 27 June 1998. The process responsible for the TIPP apparently produced some substantial LF/VLF radiation in addition to the very bright VHF radiation, so that NLDN was able to detect and geolocate it (42.97°N, 65.99°W). In Figure 2 the observations are presented after dechirping of the original FORTE-recorded signals, according to the first-order ionospheric dispersion effect ( $t \propto \text{TEC} \times f^{-2}$ ,  $t$ : group delay;  $f$ : radio frequency, e.g., [Jacobson *et al.*, 1999]). The ionospheric dispersion effects over the VHF radio signals are well known and have been described in detail elsewhere [Budden, 1985; Davis, 1990]. The dechirping techniques we use for the FORTE data analysis were reported by Jacobson *et al.* [1999]. If the signals had not been dechirped, then the lower-frequency signal components would have arrived later than the higher-frequency components. The rest of the analysis for the TIPP events is essentially the same as that presented by Shao and Jacobson [2001] for the LAPP pulses.

[11] Figure 2a shows the power spectrogram computed from the signals received by both the antennas, i.e.,  $E_1^2 + E_2^2$ , with “sliding” Fourier transforms of the dechirped time series data. The Fourier window is 64 data points (1.28  $\mu\text{s}$ ) wide and is tapered by a Hanning window. The “sliding” is done by advancing the Fourier window by 2 points (0.04  $\mu\text{s}$ ) along the time axis. The first pulse is the original pulse; and the second is the reflection off the Earth’s surface. In contrast to the LAPP observations in Figure 2 of the previous publication [Shao and Jacobson, 2001], the magnetoionic splitting [Budden, 1985; Massey *et al.*, 1998b] for each TIPP pulse is not everywhere obvious, but is well-resolved below 35 MHz.

[12] Figure 2b shows the degree of polarization  $d$  in the range of 0 to 1, which is computed from the time-averaged  $I, Q, U$ , and  $V$  for each frequency component after the same “sliding” Fourier transforms as for the power spectrogram shown in Plate 1a. The averaging interval spans 300 consecutive Fourier-window steps (12  $\mu\text{s}$ ) at 26 MHz, and the interval decreases linearly to 180 Fourier windows (7.2  $\mu\text{s}$ ) at 51 MHz. The averaging interval is also tapered with a corresponding Hanning window. It is clear that both pulses are highly polarized at frequencies below 40 MHz, with each pulse being split by an unpolarized gap. For each pulse, the two split, highly polarized regions are associated with the ordinary (fast) and extraordinary (slow) magnetoionic modes [Shao and Jacobson, 2001; Budden, 1985], which on the other hand are much less distinguishable by the power spectrogram (Figure 2b).

[13] To further illustrate the two modes, Figure 2d shows the openness of the polarization ellipses and the senses of the E-vector rotation,  $\epsilon$ , in the range of  $-45^\circ$  to  $+45^\circ$ . Similar to the LAPP observations, the ordinary and extraordinary modes of a TIPP pulse are both detected to be elliptically polarized, with the corresponding E-vectors rotating clockwise ( $\epsilon < 0$ ) and anticlockwise ( $\epsilon > 0$ ), respectively. Due to the limited color resolution in Figure 2d, the exact  $\epsilon$  value for each mode is not visually obvious. As will be shown later in Figure 3, careful examinations indicate that  $|\epsilon|$  is about  $35^\circ$

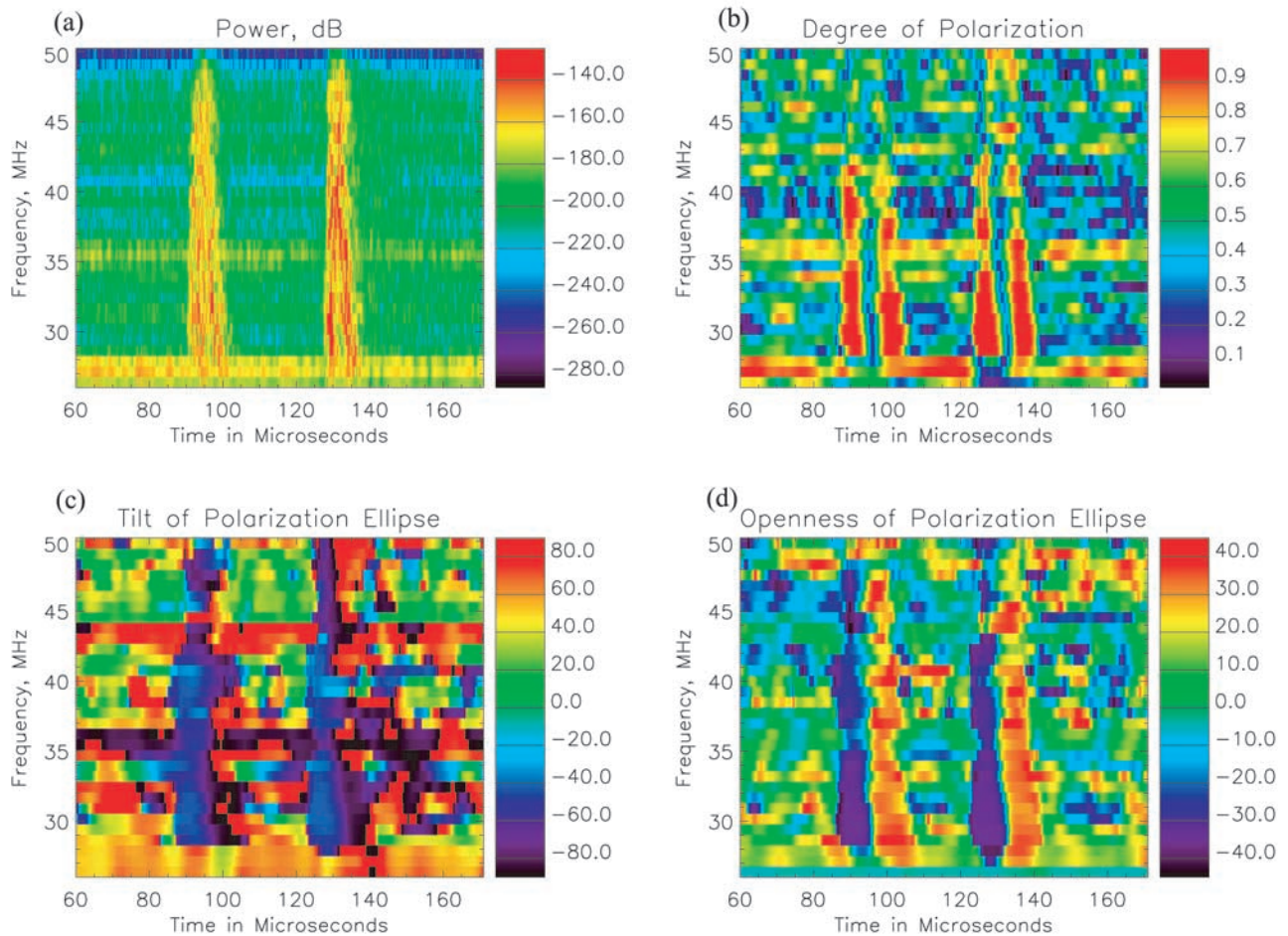


**Figure 2.** Analysis for a TIPP event after dechirping the data. (a) Spectrogram of total power from both of the LPA antennas. (b) Degree of polarization  $d$ , color-coded from 0 to 1. (c) Tilt angle of polarization ellipse, from  $-90^\circ$  to  $+90^\circ$  as referenced to the satellite's ram direction. (d) Openness of polarization ellipse, from  $-45^\circ$  to  $+45^\circ$ .

for each mode within each pulse. At VHF, each mode is expected to be circularly polarized if it were observed in the direction of the wave propagation. The departure from perfect circular polarization ( $|\varepsilon| = 45^\circ$ ) is due to the FORTE antenna patterns. For this case, the satellite was at (37.03°N, 67.27°W, 806 km), and the TIPP was at (42.97°N, 65.99°W) near the Earth's surface. Being viewed from the satellite, the TIPP was at  $40.1^\circ$  away from the nadir and  $-148.2^\circ$  away in azimuth from the ram direction. The ram direction coincides with the orientation of one of the LPA antennas, and is referred to as the positive  $x$  direction as in Figure 1. According to this geometry and the model that links the FORTE-measured polarization and the antenna beam pattern, as discussed in detail in [Shao and Jacobson, 2001],  $|\varepsilon|$  should be  $37.4^\circ$ , which closely agrees with what is actually measured.

[14] The mirror image appearance from one mode to the other suggests that the original radiation was linearly polarized, before it underwent the magnetoionic splitting through the ionosphere. The apparent unpolarized gap at the middle of each of the two TIPP pulses (Figure 2b) was due to both a gap between, and incoherent mixing of, the two temporally split modes, and so was that at frequencies

above 40 MHz. With known locations of both the source and the satellite, together with the slant TEC and the geomagnetic field, the expected temporal splitting between the two modes can be computed analytically, as described in detail in [Shao and Jacobson, 2001]. For this case, the split ( $\Delta t$ ) between the two modes was on the order of  $1 \mu\text{s}$  between 40 and 50 MHz. With the Hanning-tapered Fourier window of  $1.28 \mu\text{s}$ , the apparent resolving bandwidth ( $\Delta f$ ) is about 1.6 MHz. Based on coherence theory [e.g., Born and Wolf, 1975, p. 319], the overlap of two identical signals will become incoherent (and therefore unpolarized) as  $\Delta t \bullet \Delta f$  increases to about 1, which is the case for the mix of the two modes at frequencies above 40 MHz. The splitting increases as the radio frequency decreases. At frequencies below 40 MHz, the modes' separation ( $4 \mu\text{s}$  at 30 MHz) is wide enough that the two modes begin to separate from each other, so that at the leading and the trailing edges of the two TIPP pulses the analysis is implemented on only one of the modes.

[15] Figure 2c shows the tilt of the major axis of the polarization ellipses ( $\tau$ ) in the range of  $-90^\circ$  to  $+90^\circ$ , referenced to the ram direction ( $x$ ) of the FORTE satellite. The tilt angles associated with the two pulses are measured

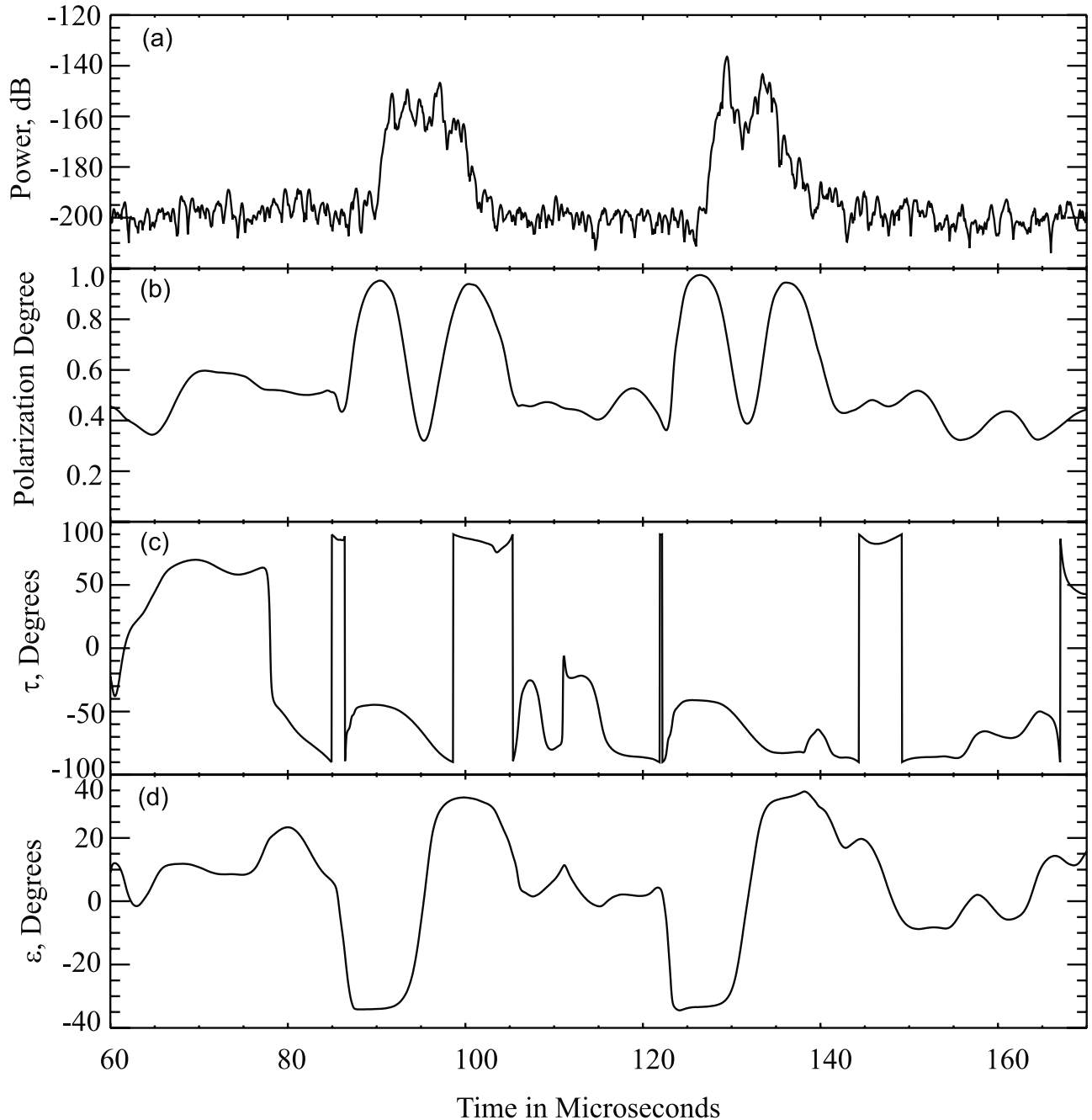


**Figure 3.** (a) Power, (b) degree of polarization, (c) ellipse tilt, and (d) ellipse openness, respectively from the top to the bottom, as averaged from Figure 2 within a 4 MHz bandwidth centered at 32 MHz.

mostly around  $-50^\circ$ , agreeing well with the prediction from the FORTE antenna model [Shao and Jacobson, 2001]. The tilt angles at the trailing edges of the two TIPP pulses are about  $\pm 90^\circ$ , far from the model prediction. It is obvious that when  $|\varepsilon|$  approaches  $45^\circ$ ,  $\tau$  is not well defined. For  $|\varepsilon|$  being about  $35^\circ$ , this could be part of the reason for the uncertainty of the  $\tau$  measurement. The other source for the  $\tau$  uncertainty could be the signal contaminations from the ordinary to the extraordinary mode.

[16] As shown in Figure 2, all the polarization properties appear nearly the same for the original and the reflected pulses. This is because (1) a polarized signal will still be polarized after being reflected from the Earth's conducting

surface, and (2) the two pulses propagate along essentially the same path through the ionosphere. The latter is justified by the fact that the source of the radiation is very near to the Earth surface as compared to the altitude of the satellite. This is true for all the lightning-produced signals. Based on the two dimensional NLDN location of the event, the instantaneous position of the satellite, and the time lag between the two pulses (about  $35 \mu\text{s}$ , Figure 2a), the height of source is found to be 8.0 km above the reflecting surface.

### 3.2. Statistical Properties of the Selected TIPP Events

[17] Having given a detailed description for the forgoing case study we progress to examine the polarization proper-

ties statistically for the 313 geolocated, VHF-bright TIPP events. Similarly to the presentations in [Shao and Jacobson, 2001] for the LAPP pulses, average values within a 4 MHz sub-band centered at 32 MHz are computed for each of the four parameters (power,  $d$ ,  $\tau$ , and  $\epsilon$ ). The sub-band is so chosen to maximize the mode separation, and to minimize the carrier interference. For the purpose of statistical study, the sub-band-averaged values are used as representative values for each individual TIPP event.

[18] Figure 3 shows the time variation of the sub-band-averaged power, degree of polarization ( $d$ ), tilt of the ellipse ( $\tau$ ), and ellipse openness ( $\epsilon$ ), respectively, for the same TIPP event shown in Figure 2.

[19] For each of the original and the reflected pulses, we select the first peak of the degree of polarization  $d$  (corresponding to the ordinary mode in each pulse) as a representative measure of  $d$  for each of the TIPP pulses. The  $\tau$  and  $\epsilon$  values that are associated with the selected peak  $d$  values are then chosen as the representative measures for the corresponding properties, respectively.

[20] We first discuss the observations for the degree of polarization, which indicates whether the radiation source is well organized, or consisting of multiple emitters, randomly oriented. As seen in Figure 2b and Figure 3b, the TIPP radiation is highly polarized with the corresponding peak  $d$  equal to about 0.95, well above the background level of about 0.5. For entirely random, unpolarized background noise, one would expect the corresponding  $d$  equal to 0. The offset of the background level is mostly due to the finite size of the Fourier window and the subsequent averaging interval applied to the data analysis. These effects will be discussed in detail in a later section. For now, we consider only the relative level of polarization compared to the measured background.

[21] Figure 4 shows the statistics for the observed  $d$  for the 313 TIPP events. The solid line in Figure 4a shows the normalized distribution for  $d$ , including both the TIPP pulses and the background noise, of the 313 sub-band-averaged records (Figure 3b). Each of the records is 200  $\mu$ s long (Figure 3 shows only a portion of the records, about 110  $\mu$ s near the TIPP pulses) and contains 5000 processed samples for the corresponding polarization parameter. The total number of  $d$  samples that make up the solid line is then 1565000. This quasi-normal distribution has a mean of about 0.5, and a level tail at  $d > 0.8$ . The dashed and dotted lines in Figure 4a show the normalized distributions for the 313 peak  $d$  values (as shown in Figure 3) for the original and the reflected TIPP pulses, respectively. Compared to the solid line, the TIPP pulses have a clear tendency toward high degree of polarization.

[22] Figure 4b helps to show the confidence level at which a TIPP pulse can be considered polarized. For each of the 313 sub-band-averaged records (e.g., Figure 3b) for  $d$ , a mean  $\langle d \rangle$  and a standard deviation  $\sigma(d)$  are computed. The peak  $d$  value that represents each of the two TIPP pulses is then compared with  $\langle d \rangle$  and  $\sigma(d)$  in terms of  $\rho = |d_{TIPP} - \langle d \rangle| / \sigma(d)$ . Figure 4b shows the distribution of the fraction of the total TIPP events that has a  $\rho$  value greater than a certain number, for the original (dashed line) and reflected (dotted line) pulses, respectively. We found that 40% of the original pulses have peak  $d$  values at least  $3.3\sigma(d)$  above the corresponding means  $\langle d \rangle$ . The probability for this to happen

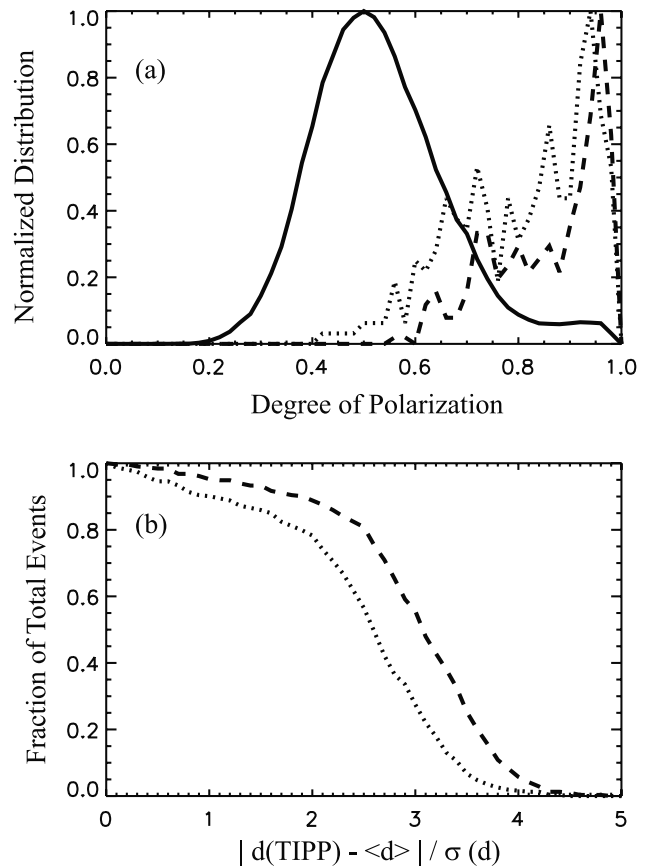


**Figure 4.** (a) Normalized distributions of background polarization level (solid line), polarization peaks of the original (dashed line) and the reflected (dotted line) pulses of the TIPP pairs. (b) Fraction of total TIPP events exceeding the polarization departure-from-mean given by abscissa. The original and reflected pulses are illustrated by dashed and dotted lines, respectively.

accidentally is less than  $4.8 \times 10^{-4}$  (assuming the  $d$  values in each record follow a normal distribution), which is equivalent to 2.4 samples in each of the 5000-sample records. It is very likely that the extraordinary mode will also have a comparable peak degree of polarization in addition to that of the original mode (Figure 3). Therefore we can conclude with full confidence that 40% of the selected TIPP events are well polarized, as compared to the background level.

[23] We also notice that the reflected pulses are commonly less polarized than the originals, as evident in both Figures 4a and 4b. This is probably due to the roughness of the reflecting surface. In any model of specular reflection, the reflected wave would be expected to be more or equally polarized. If the surface is rough compared to the radian wavelength ( $\lambda/2\pi$ , about 1–2 m in our case), the composite of the reflected signals will add up incoherently, and will degrade the degree of polarization.

[24] Figure 5 shows the dependence of the peak degree of polarization upon the magnetoionic mode splitting for the original TIPP pulses. As having been discussed earlier for Figure 2, with the known positions of the satellite and the radiation source, together with the slant TEC and the geo-

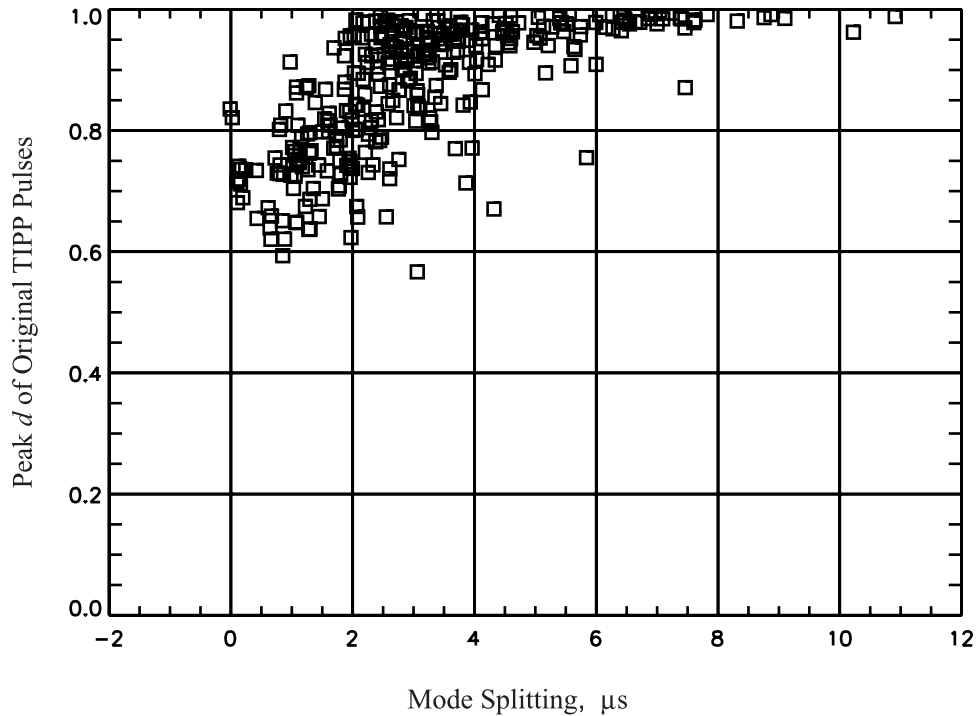


**Figure 5.** Dependence of peak polarization upon the predicted mode splitting at 32 MHz. The splitting is computed from the known TIPP and satellite positions, the TEC, and the geomagnetic field.

magnetic field, the expected mode splitting can be estimated theoretically [Shao and Jacobson, 2001]. For splitting greater than 4  $\mu\text{s}$  the TIPP pulses are observed with high degree of polarization (between 0.9 and 1) and the degree of polarization appears independent of the splitting. With the splitting less than 4  $\mu\text{s}$ , the degree of polarization follows a general decreasing trend as the splitting decreases. As discussed earlier for the case study (Figure 2), the observed decline of  $d$  for narrower splitting is apparently caused by the overlapping of the two modes. The less the splitting, the more the polarization is corrupted, if the signal has a duration greater than the splitting. However, as the split narrows further to the “intrinsic coherence time” ( $\Delta t \sim 1/\Delta f$ ) the two modes will start to mix coherently. In this situation, the measured polarization will start to increase, only if, however, the original source is polarized. For the analysis in this paper, the Fourier window is 1.28  $\mu\text{s}$  and is tapered with a Hanning window, so the effective resolving bandwidth  $\Delta f$  is about 1.6 MHz, which leads to 0.6  $\mu\text{s}$  for the “intrinsic coherence time”  $\Delta t$ . In Figure 5, there exist a few observations that have mode splitting narrower than 0.6  $\mu\text{s}$ , and the corresponding  $d$  for these events appear to reverse the main decreasing trend, indicating they were originally polarized. Having shown the effects of splitting on the measured polarization, we infer that most of the 313 TIPP pulses were probably originally polarized. The previous firm assertion for 40% of the events was, therefore, overly conservative.

[25] Except for the apparent splitting dependence, the degree of polarization is found not to depend on the peak power, the pulse width, or the source height for the selected TIPP pulses. The TIPP pulses in this paper span a range of peak power over 10 dB, and have apparent pulse widths of up to a few

microseconds. The heights of the TIPP pulses are found mostly in the range of 7–15 km above the ground surface, as estimated from the NLDN-determined horizontal locations and the time lags between the pairs of the TIPP pulses.

[26] Following similar steps as were developed for the investigations for the LAPP pulses [Shao and Jacobson, 2001], we now report observations for the openness of the polarization ellipse ( $\epsilon$ ) and the tilt of the corresponding major axis ( $\tau$ ), for the split modes. To do this, we select only the TIPP pulses that were detected with high degree of polarization, and will examine only the ordinary mode (the extraordinary mode will appear as a mirror image) for each of the pulse pair. For TIPP pulses with lower degree of polarization, which is apparently due to the incoherent merging of the two modes, the actual  $\epsilon$  and  $\tau$  will be corrupted, and the measured values cannot be used in the following.

[27] Figure 6 shows the  $\epsilon$  observations for TIPP pulses with  $d > 0.85$ . There are total of 183 such events. As described in detail by Shao and Jacobson, [2001], at VHF, each split mode should be circularly polarized ( $|\epsilon| = 45^\circ$ ) as being viewed in the wave normal direction. With the beam pattern of the FORTE antennas, the arriving polarization circle will be foreshortened toward an ellipse. The measured  $\epsilon$  depends predominantly on the angle away from the satellite’s nadir, and slightly on the angle of azimuth referenced to the satellite’s ram direction, as viewed from the satellite. Figure 6 shows the nadir angle effect on the measured  $\epsilon$  for the ordinary modes for both the original and the reflected pulses. For the ordinary mode, the  $E$  vector rotates clockwise, as viewed over the Earth’s northern hemisphere. In the figure, we present  $\epsilon$  for the original TIPP pulses by their actual values (all the data points with negative values), and reverse the signs for the reflected pulses (so they appear as

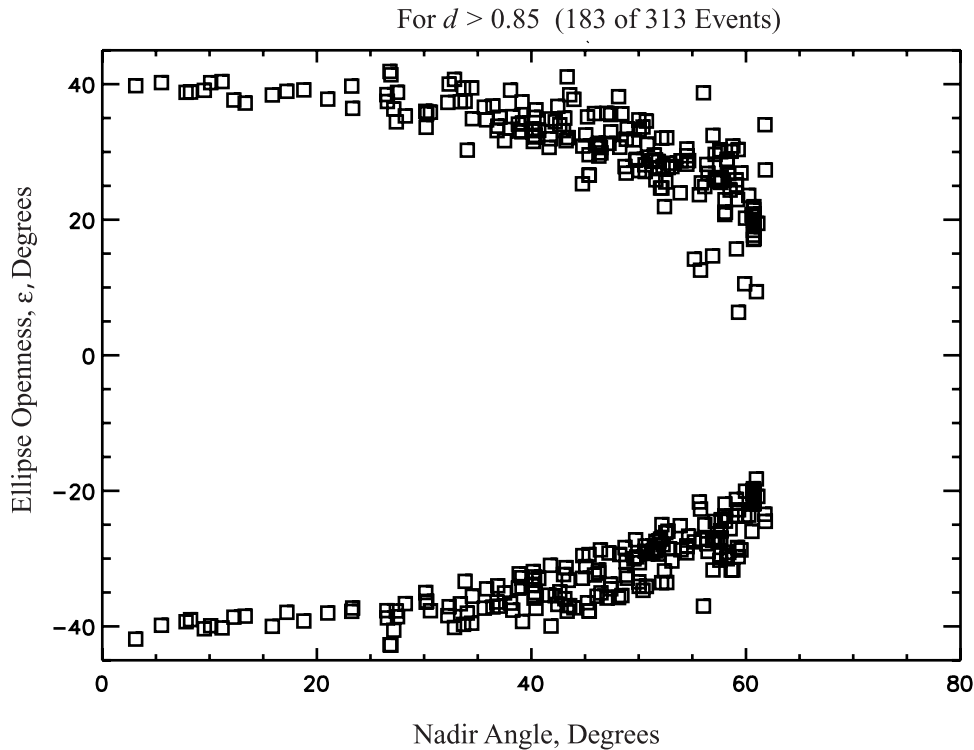


**Figure 6.** Dependence of ellipse openness  $\epsilon$  on the angle away from the satellite nadir. Observations of only the ordinary mode are shown. The lower half and the upper halves are for the original and reflected pulses, respectively, with the latter being reversed in sign.

positive values), so that they can be shown and compared in the same plot. Same as we found for the LAPP observations, for sources nearly straight underneath the satellite, the pulses are found to be nearly circularly polarized ( $|\epsilon| = 45^\circ$ ); while for sources at increasingly larger nadir angles, they are foreshortened more toward elliptical polarization, agreeing with the predictions from the FORTE antenna beam pattern. Since the heights of the TIPP sources are typically 7–15 km above the ground, which is small compared to the height of the satellite, the satellite will view each pair of the TIPP pulses as arriving from the same direction. In the worst case, the direction will differ no more than  $2^\circ$  for a pair. As shown in Figure 6,  $\epsilon$  for the reflected pulses appears slightly noisier than the originals, but is consistent in general with the originals, indicating each pair arrives to the satellite from about the same direction.

[28] For the tilt of the polarization ellipse  $\tau$ , we loosen the degree-of-polarization criteria to  $d > 0.80$ , but select only those events that have  $|\epsilon|$  less than  $35^\circ$  for the original pulses. It is obvious that for nearly circular polarization ( $|\epsilon| \sim 45^\circ$ ), the major axis will not be well defined, and therefore the corresponding  $\tau$  will not be measured accurately. Under the two selection criteria, there remain a total of 144 of the 313 TIPPs. Figure 7a shows the observations of  $\tau$  at various azimuths for the original pulses of the 144 TIPPs. The solid line indicates the expected tilts computed from the beam pattern of the FORTE antenna [Shao and Jacobson, 2001]. It is clear that the observations agree very well with the antenna model predictions, and the orientation for each ellipse forms a right angle to the arrival direction of the wave. Since the polarization analysis can only resolve

the tilt in the range  $-90^\circ$  and  $+90^\circ$ , the measured  $\tau$  will appear the same for waves arriving from two opposite directions. Figure 7b shows the same observations for the reflected pulses. Similar to the  $\epsilon$  observations, measures of  $\tau$  for the reflected pulses are a little noisier than, but in general agree well with, those for the original pulses, consistent with the fact that each TIPP pair is from the same azimuthal direction.

#### 4. Observations of other Types of Lightning Processes

[29] The TIPP events we have reported so far appear to be a signature of a very special type of in-cloud discharges. In this section we will report polarization observations for some other types of lightning processes, closer to those more commonly observed by ground-based experiments. For this study, we will present the observations over the Earth’s equatorial region. Over the equatorial region, the line-of-sight between a terrestrial signal and the satellite is more likely to form a large angle to the vector of the geomagnetic field, and moreover the magnitude of the geomagnetic field at the effective ionosphere height is smaller by at least 15% than that at the midlatitude. These two effects help to minimize the magnetoionic splitting between the two modes [Shao and Jacobson, 2001], and therefore to increase the possibility of coherent overlap between the two modes. This is particularly important for investigations of continuously radiating processes (e.g., leaders), which otherwise can be substantially contaminated

For  $d > 0.80$ ,  $|\varepsilon| < 35$  deg (144 of 313 Events)

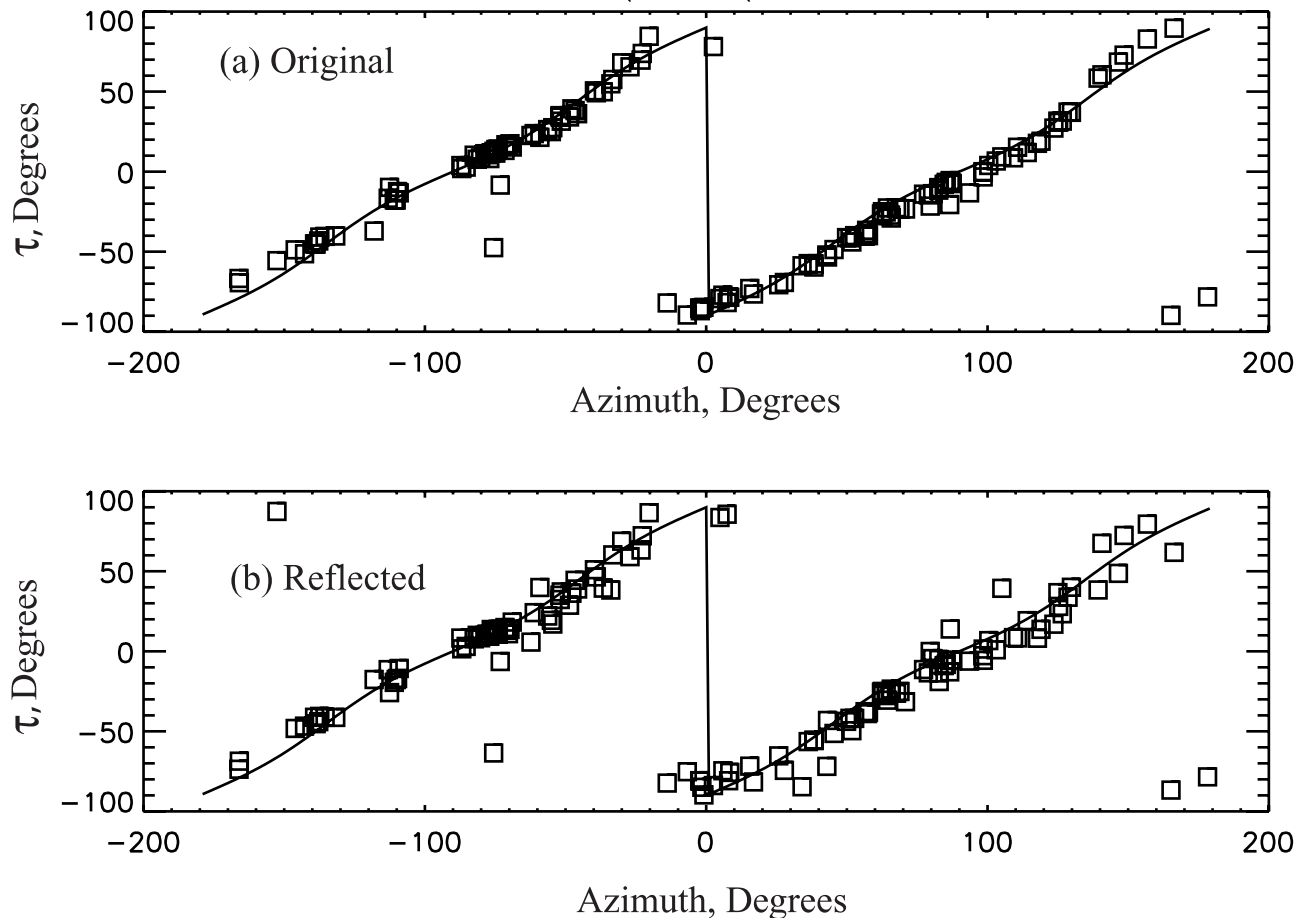


**Figure 7.** Relation between the measured tilt of polarization ellipse and the arriving azimuthal angle for the (a) original and (b) reflected pulses. The solid line is from the model based on the antenna beam pattern [Shao and Jacobson, 2001].

by the constant incoherent overlap of the widely split modes.

#### 4.1. Sequence of Brief Radiation Pulses

[30] Sequences of impulsive VHF pulses have been observed typically at the beginning of lightning flashes, and often during the development of the flashes [e.g., Proctor *et al.*, 1988; Shao and Krehbiel, 1996]. In either case, the pulses are associated with virgin air breakdown processes that usually contribute to new channel development. The VHF-intense TIPP, on the other hand, often appear isolated in time and not associated with normal lightning discharges [Jacobson *et al.*, 1999; Smith *et al.*, 1998].

[31] Figure 8 shows polarization observations for a portion of such a sequence. During a time period of 92 ms, the FORTE radio receiver had been triggered 11 times consecutively. Within each triggered record (400  $\mu$ s in length, as typical for the FORTE data acquisition), multiple pulses similar to that shown in Figure 8 are observed. Figure 8 corresponds to the third trigger in this series of pulses, and is about 13 ms into the trigger sequence. This sequence of pulses was observed on 13 September 1999 between

17:14:12.112 and 0.204 UT, when the satellite was over the equatorial region (3.1°S, 154.0°E). There was no simultaneous ground-based observation for this sequence, and therefore the exact type of its parent lightning flash cannot be determined. However, an initial-type of negative ground stroke followed the sequence within 77 ms, as will be discussed below, suggesting the sequence is a part of a -CG flash.

[32] The analysis for Figure 8 is essentially the same as for Figure 2, except (1) the data is not pre-dechirped and (2) the “sliding” Fourier window contains 256 data points instead of 64. None of the six pulses indicates any obvious mode splitting, in contrast to the midlatitude TIPP. Compared to the background, the initial four pulses are somewhat polarized (Figure 8b), while the last two are just barely distinguishable from the background.

[33] The observations of the tilt of the polarization  $\tau$  (Figure 8c) for the two middle pulses reveal very clearly the so-called Faraday-rotation phenomenon [Budden, 1985; Davis, 1990; Shao and Jacobson, 2001]. The tilt rotates continuously as frequency varies, as indicated by the periodic color changes, and the rotation rate decreases gradually at higher frequencies, consistent with the  $f^{-2}$

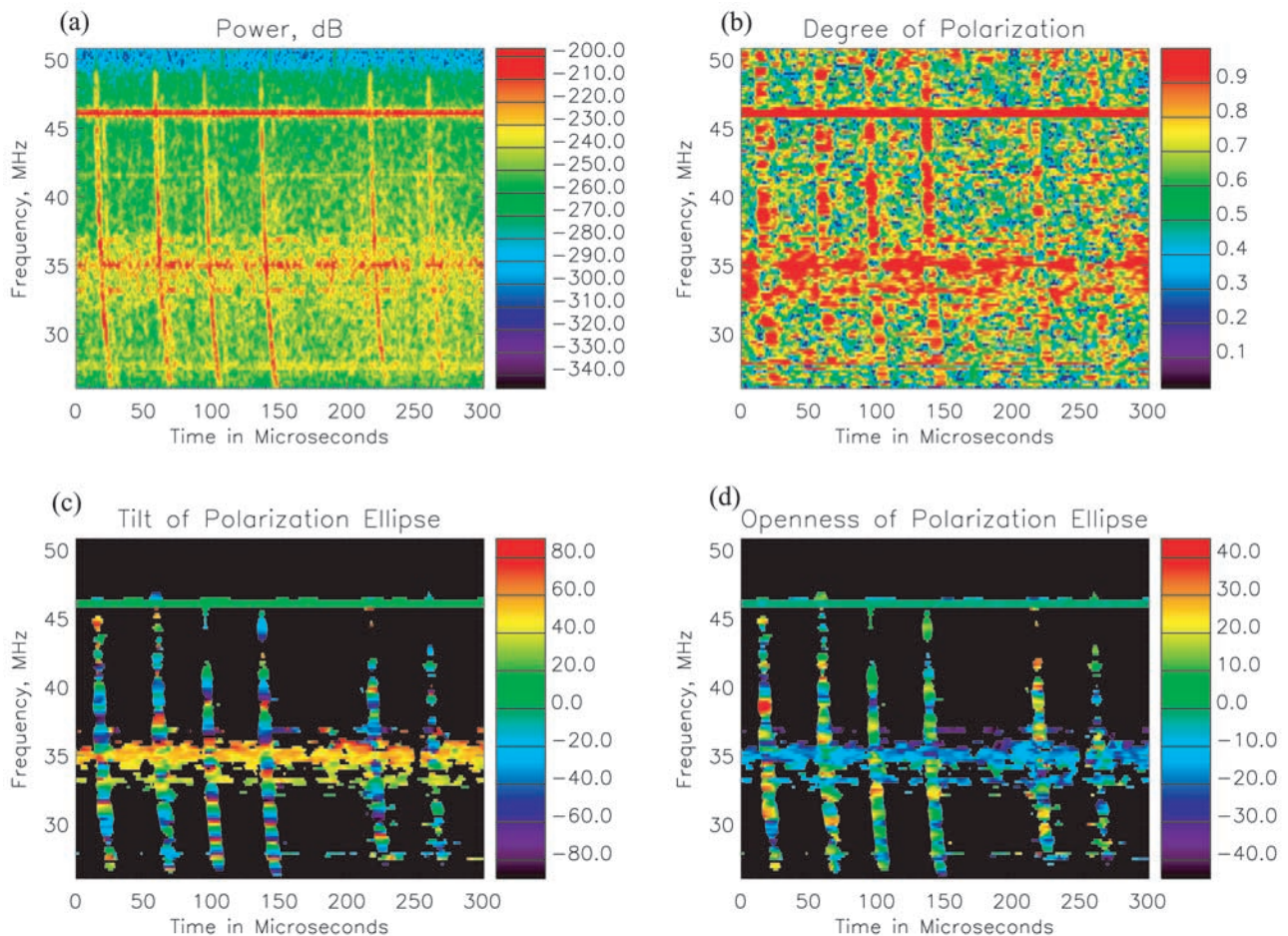


**Figure 8.** Same as Figure 2 but for a series of pulses occurred 13 ms into a 92 ms sequence, which is apparently associated with a normal  $-CG$ . The record was obtained over the equatorial region with no evident mode splitting. Faraday rotation is detected instead.

dependence based on the ionospheric theory. The rest of the pulses in this record cannot be detected with evident, consistent Faraday rotations, due to their being less polarized. Detailed discussions on frequency-dependent Faraday rotation for broadband signals have been presented in our previous paper [Shao and Jacobson, 2001].

[34] Figure 8d shows the corresponding openness of the polarization ellipse. The two middle pulses are detected mostly linearly polarized ( $\epsilon \sim 0^\circ$ ). Since the observation was conducted over the equatorial region, the two magneto-ionic modes can be considered as arriving at the satellite simultaneously; the observed polarization should then reveal the source polarization, except, of course, for the  $E$  plane Faraday rotation. Therefore, the source radiation for the two pulses must be linearly polarized. This is consistent with the corresponding  $\tau$  observations, for the reason that only nearly linear polarization at the source can be detected with clear Faraday rotations. The linear polarization is similar to that of the TIPP events, although for the TIPPs we inferred the linear polarization from the two separate, mirror-imaging elliptical modes.

[35] The fact that the two middle pulses appear the same in terms of polarization indicates that the second of the pair is the ground reflection of the first, just as in a TIPP event. It

is also reasonable to infer that the first and the third pairs in the record are also pairs of TIPP-like events, for that they have about the same inter-pulse time lags as the middle pair.

[36] Besides the lightning radiation, we note a strong carrier signal at 46 MHz. The carrier is highly polarized with linear polarization.

[37] The other 10 records in this FORTE trigger sequence have shown similar polarization properties. For instance, Figure 9 shows the spectrograms of the power and the degree of polarization for the 9th record, 82 ms into the beginning of the sequence. This record contains three recognizable pulses and their corresponding reflections. The two radiation intense pulses and the reflections are detected polarized.

#### 4.2. Initial Stroke to Ground

[38] As mentioned above, the pulse sequence of Figure 8 was followed 77 ms later by an initial-type of negative stroke to ground. The FORTE receiver was triggered at 17:14:12.281 UT by VHF signal associated with the stroke, and its observations are shown in Figures 10a and 10b. Although it is uncertain whether the previous pulse sequence and this stroke belong to the same flash, the facts that they occurred close together in time and

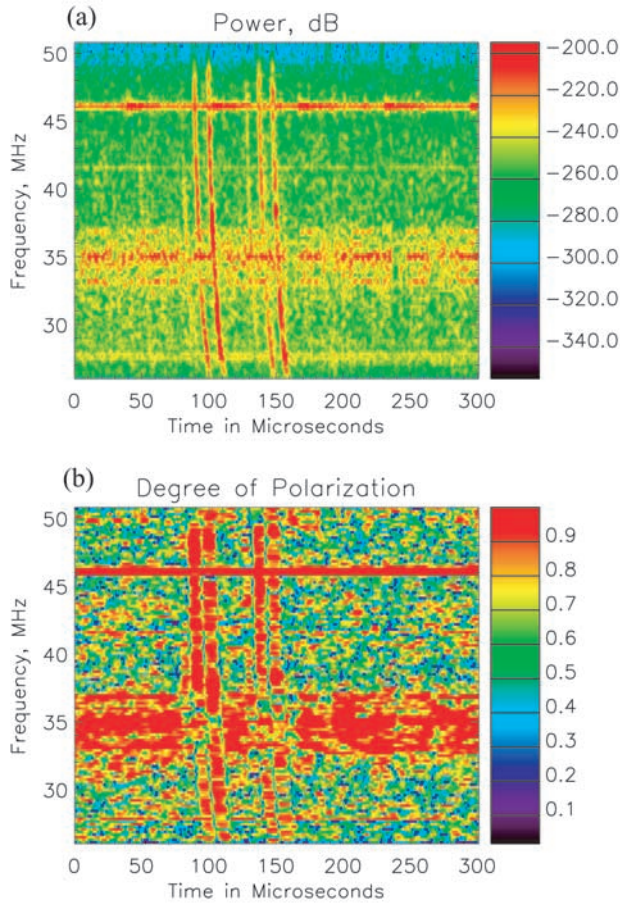


**Figure 9.** Another example series 82 ms into the same sequence. Only the power and degree of polarization are shown.

appear to have the same degree of ionospheric dispersion (as shown by the power spectrograms) suggest they might. The identification of the initial stroke from this FORTE record is based on the behavior of its radiation power. As from previous ground-based [Rhodes *et al.*, 1994; Shao *et al.*, 1995; Shao *et al.*, 1999] and FORTE observations [Suszcynsky *et al.*, 2000] for initial strokes, the radiation power is typically enhanced significantly at the instant when the return stroke starts, as compared to pre-stroke radiation, and then decays gradually in the following few hundreds of microseconds. The power observation of Figure 10a is in agreement with the characteristics of an initial stroke as the return stroke occurs at about 100  $\mu$ s into the record. As readily seen in Figure 10b, no polarization (or, in other words, random polarization) is detected for the entire record that includes 100  $\mu$ s of leader process and about 200  $\mu$ s of return stroke and post-stroke processes. The corresponding observations for  $\tau$  and  $\epsilon$  for this completely unpolarized signal are just noise-like, and therefore are not shown here.

[39] Just to illustrate further the observations for initial strokes, Figures 10c and 10d show another similar example. This initial stroke was recorded on 11 September 1999 at 19:43:21.998 UT, when the satellite was also over the equatorial region (4.8°N, 125.7°E). As with the previous initial stroke, there is no sign of polarization detected in the

VHF. Other FORTE-detected initial strokes we have analyzed show similar polarization features.

### 4.3. Dart Leader and K-Type Streamer

[40] About 8 s prior to the second example of the initial strokes shown in Figure 10, at 19:43:13.750 UT on 11 September 1999, the FORTE satellite was triggered by an apparent dart leader to ground. Again, the type of the discharge process is inferred from the properties of its radiation power. As shown in Figure 11a, the radiation was continuous and then ceased sharply, typical for a dart leader that begins a subsequent stroke to ground. As shown in Figure 11b, there is no recognizable polarization detected for the dart leader process.

[41] Figures 11c and 11d show observations for an apparent K-type streamer. This K-type discharge occurred at 19:43:09.968 UT, about 4 s before the just discussed dart leader. The breakdown process for K streamers is essentially the same as that for a dart leader to ground, as reported with ground-based VHF interferometer observations [Rhodes *et al.*, 1994; Shao *et al.*, 1995; Shao and Krehbiel, 1996], except they stop inside the cloud rather than reaching the ground. As for the dart leader, the K streamer is also observed with no polarization.

## 5. Discussion

[42] We have so far examined the degree of polarization rather qualitatively for the TIPP, as well as for the other type of discharge events, as referenced to the computed polarization level for the background noise. As briefly pointed out before, for entirely randomly polarized background noise, one would expect the corresponding  $d$  equal to 0. Figures 2b, 3b and 4a all have shown that the background level is rather high. For the 313 TIPP events, the mean background level is about 0.5, as shown by the solid line in Figure 4a. The reason for the elevated background level is mostly due to the finite size of the Fourier window and the subsequent averaging interval implemented in the data analysis. To have balanced frequency and time resolutions, the Fourier window and the time-averaging interval have to be chosen with a finite, optimal number of data samples. The Stokes parameters in Equation 1 are in fact the measures of coherence between the two orthogonal electric field components of the incident wave. Obviously, with a finite number of data samples (e.g., finite averaging interval) even entirely random signals will appear to have some degree of coherence, either auto-coherence for one signal or cross-coherence between signals. To better understand the implication of the  $d$  observations, Figure 12 shows its modeled dependences upon the Fourier window size and the averaging interval for two independent, normally distributed random signals, so as to simulate a completely unpolarized wave. For a chosen Fourier window (and therefore an apparent resolving frequency bandwidth),  $d$  decreases with increasing time-averaging interval; while for a chosen averaging interval,  $d$  decreases with decreasing Fourier window size (increasing apparent bandwidth). For the TIPP analysis presented in this paper, the Fourier window and the averaging interval are chosen as 64 data points (resolving bandwidth: 1.6 MHz) and 12  $\mu$ s, respectively. The corresponding  $d$  computed for a random,

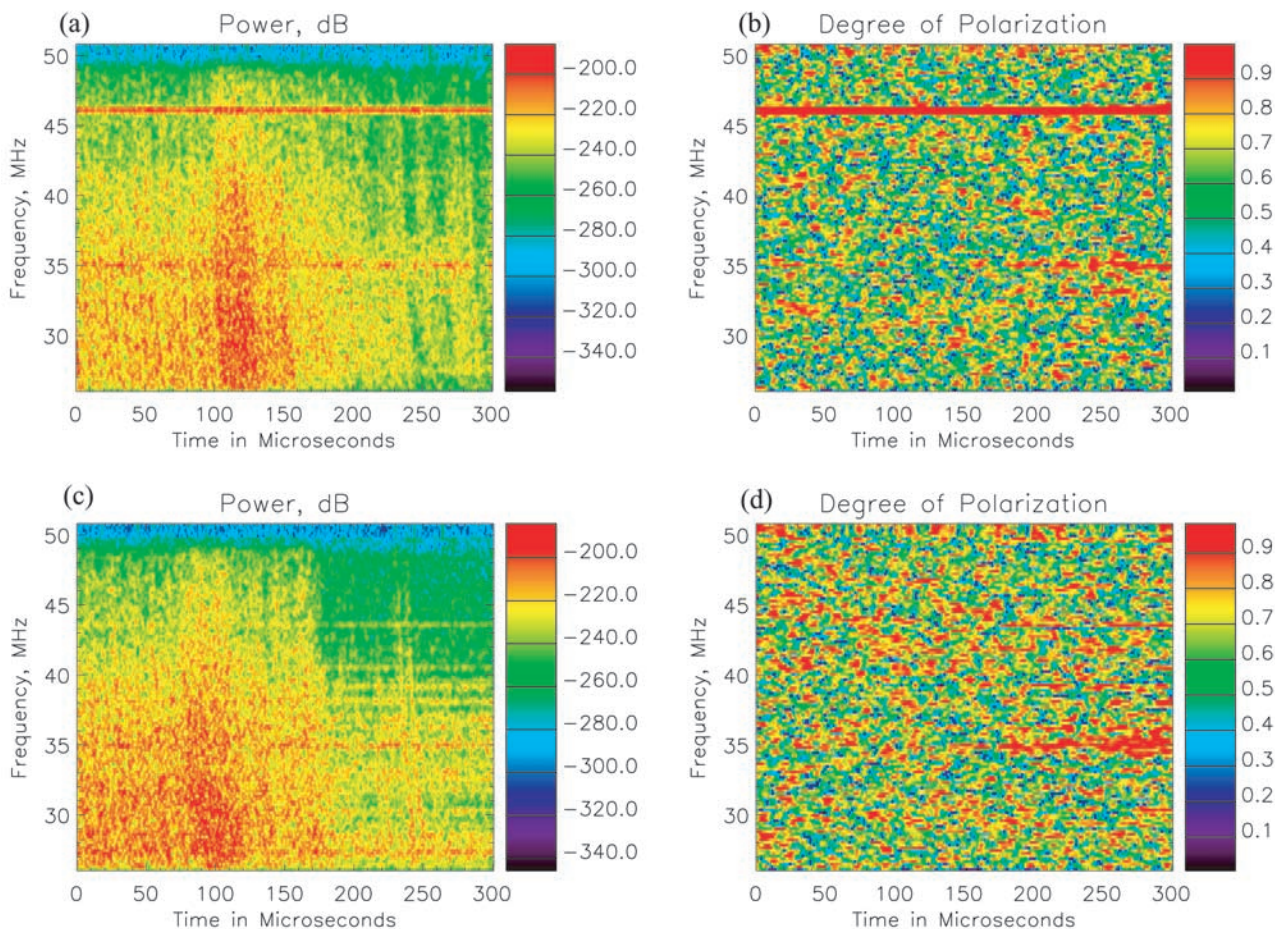


**Figure 10.** Two examples of VHF associated with initial strokes. Both observed over the equatorial region. Only power and degree of polarization are shown. No polarization is detected near the strokes.

unpolarized signal is expected to be about 0.3. Signals with an observed  $d$  greater than the expected background level can be considered as polarized. The mean background level for the TIPP events is apparently greater than the random value 0.3, indicating that the selected 4 MHz sub-band may sometimes contain carriers, which are usually well polarized.

[43] Having discussed the expected background level with certain sizes of Fourier window and averaging interval, we now examine the significance for the computed degree of polarization for signals that override the background noise. To do this, we first generate two independent series of normally distributed noise to simulate the background for the  $x$  and  $y$  components, as for Figure 12, and then add a coherent, polarized signal to each of the series. The degree of polarization is then computed at different signal power levels. The theoretical value of the degree of polarization can be determined by comparing the signal power to the background noise power, that is  $d = P_{signal} / (P_{signal} + P_{noise})$ , and the computed value can be obtained through the same processes as for the actual data analysis, with Fourier window of 64 points and averaging interval of 12  $\mu s$ , same as that for the TIPP analysis, Figure 13 shows the computed versus the theoretical random  $d$ . For purely noise background, for which the expected  $d$  should be 0, the computed  $d$  is found to be about 0.3, agreeing with that shown in

Figure 12. As the signal power increases (so as the expected degree of polarization), the computed  $d$  increases rather slowly when the signal power is no more than 70% of the total power and then very steeply thereafter. The slow increase at the beginning is apparently due to the competing of the noise with the signal. Furthermore, for most polarized signals, the actual degree of polarization will likely be underestimated, also due to the composite of the background noise and the signal.

[44] Among the 313 TIPP events, 225 were detected with degree of polarization greater than 0.8, which is corresponding to about 0.95 for the actual fraction of the polarized power, as seen in Figure 13. Accounting for the mode-splitting effects, there will be more TIPPs that actually have the polarization level greater than 0.8. The implication of the high degree of polarization is obvious, that the breakdown processes that produce the VHF radiation are highly organized. For linear polarization, which should be the case for the TIPP radiation as would be detected without the ionosphere, the radiating current element is linear and quasi-unique.

[45] On the other hand, radiation produced by initial strokes, dart leaders and K streamers are detected with no recognizable degree of polarization. We noticed that the radiation for these events is somewhat continuous. To understand the polarization observations for the continuous

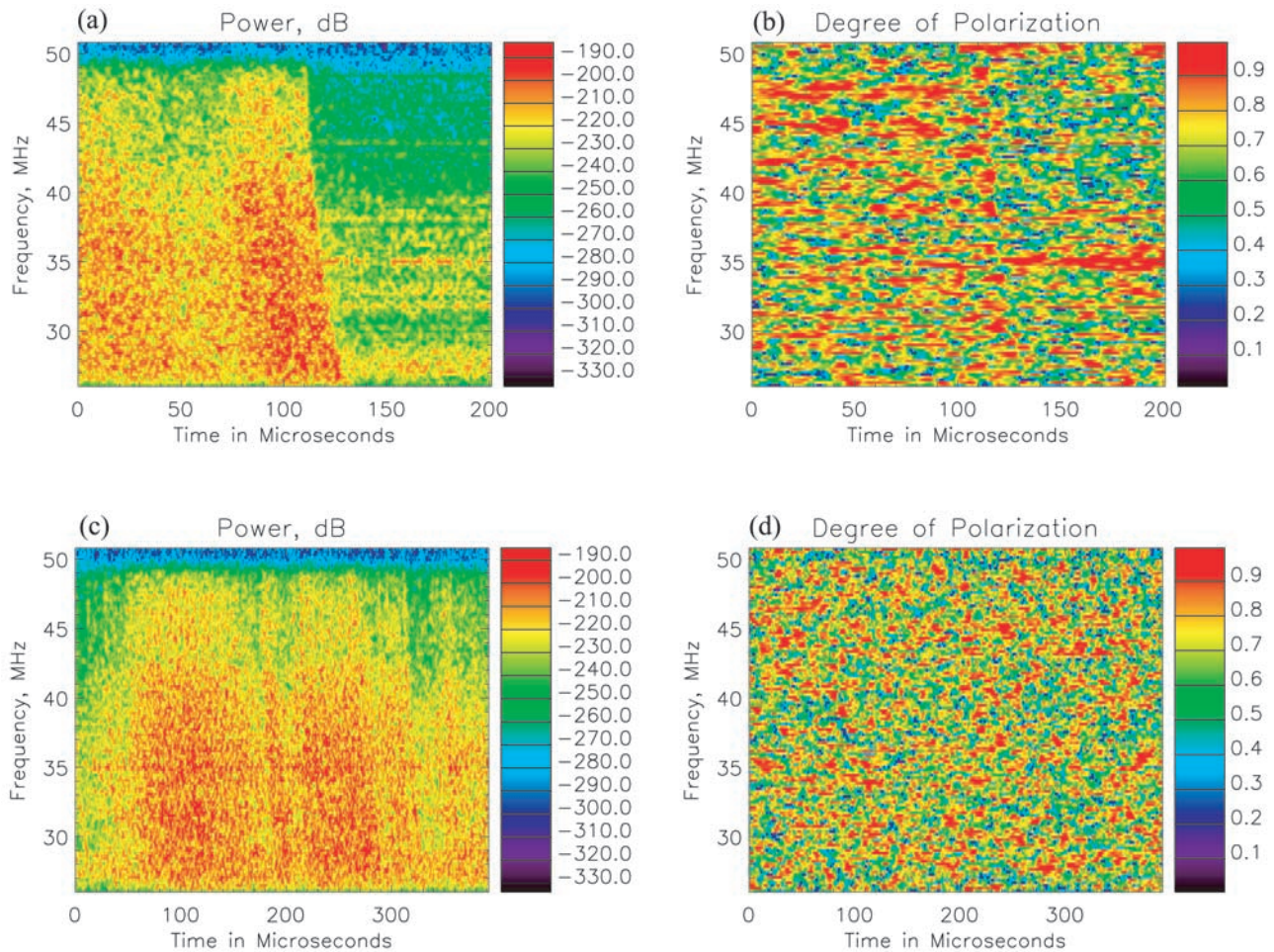


**Figure 11.** Similar to Figure 10, but observations of a dart leader and a K streamer. No recognizable polarization is detected.

radiation, the effects of the temporal averaging need to be more carefully examined. The nominal interval for the time averaging used in this analysis is 12  $\mu\text{s}$ . Being weighted with a corresponding Hanning window, the effective interval is about 6  $\mu\text{s}$ . For the continuously radiating leaders and K streamers, the measure of the polarization is therefore an average for an ensemble of potentially many individual breakdown processes that occur within the time interval. For the last stage of an initial leader to ground, for instance the first 100  $\mu\text{s}$  in Figures 10a and 10c, a significant number of stepped-like breakdown processes can happen during a 6  $\mu\text{s}$  interval. During this stage, many branches progress simultaneously, and the branches will follow a variety of directions. Thus, it is not surprising to detect no polarization from this stage. The return stroke propagates upward along the main channel, and at the same time re-explores the multiple branches [Rhodes *et al.*, 1994; Shao *et al.*, 1995], and its radiation is thus not expected polarized either.

[46] A dart leader or a K streamer follows a well-defined, pre-ionized channel. Within a 6  $\mu\text{s}$  period, the corresponding radiation sources will propagate continuously forward a few meters to a few tens of meters, at the speed of  $10^6$  to  $10^7$   $\text{ms}^{-1}$  [Rhodes *et al.*, 1994; Shao *et al.*, 1995; Shao and Krehbiel, 1996]. The observations of no preferred polar-

ization could be due to the tortuosity of the channel geometry. For instance, *Idone* [1995] (also see other reports reviewed in that paper) reported that channels to ground have significant tortuosity on a spatial scale of  $\sim 10$  cm. If the orientation of the breakdown process continuously follows a direction of the tortuous leader channel down to a 10 cm scale, the polarization as integrated over a few to a few tens of meters could result as purely random and unpolarized. However, if the 10 cm scale tortuosity can be ignored, the channel of a dart leader appears to be rather smooth in the scale from meters to tens of meters (see review in *Uman* [1987]). If the breakdown process that produces the VHF radiation is also in the meters to tens of meters scale (comparable to the scale of the VHF wavelength), one would expect the detected radiation to be polarized. The other possible mechanism for the VHF unpolarized dart leader and K streamer could be due to the peculiar electric field environment near the tip of the leader. As depicted by *Borovsky* [1995], a significant portion of the electric field points radially inward to the leader channel. If the breakdown process follows the directions of the electric field and are oriented radially around the leader tip, the produced VHF radiation will be viewed as purely unpolarized.

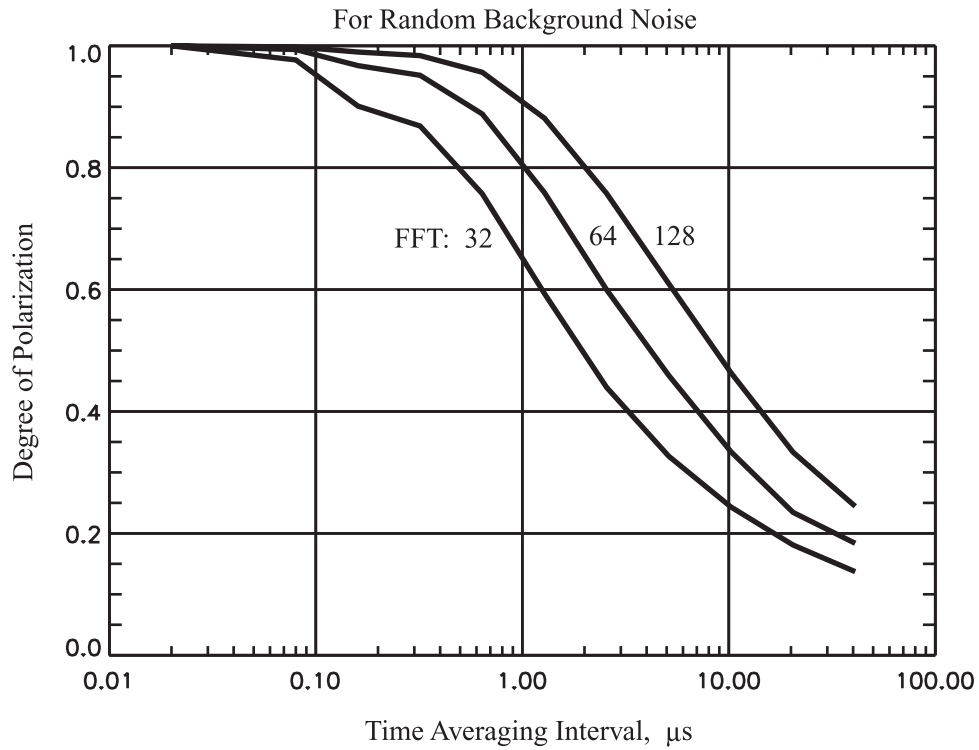


**Figure 12.** The expected background level of degree of polarization for normally distributed random noise. The expected level is dependent on the sizes of both the Fourier window and the time-averaging interval.

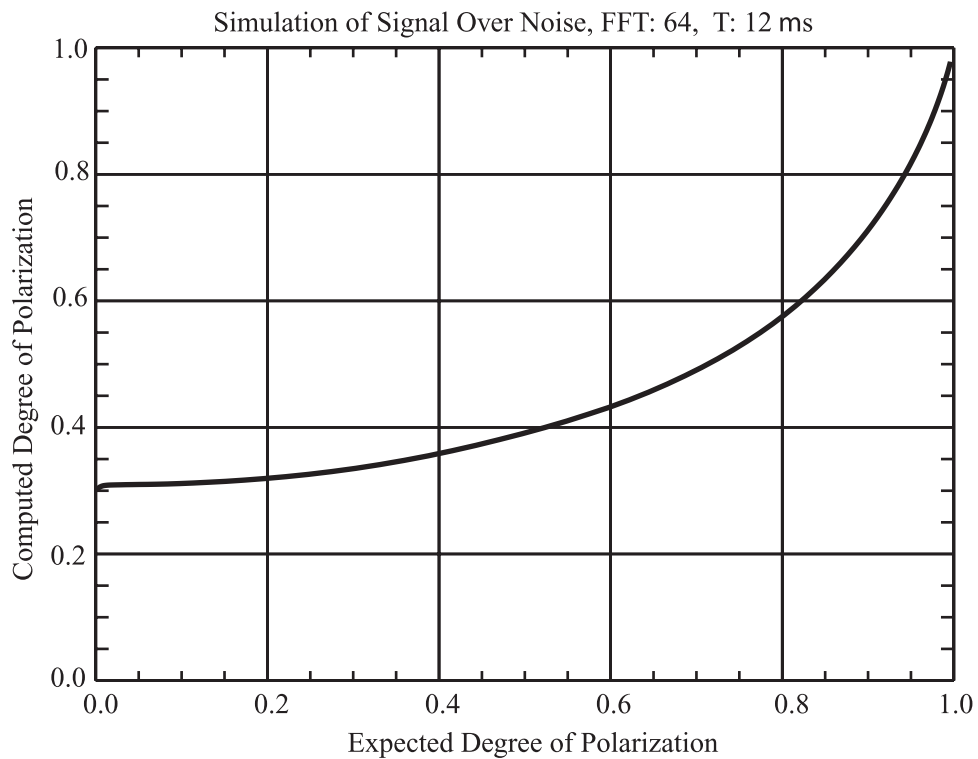


**Figure 13.** The significance of measured degree of polarization for polarized signals riding over random background noise. The horizontal axis indicates the actual fraction of polarized power over the total power, while the vertical axis indicates the computed (or measured) degree of polarization.

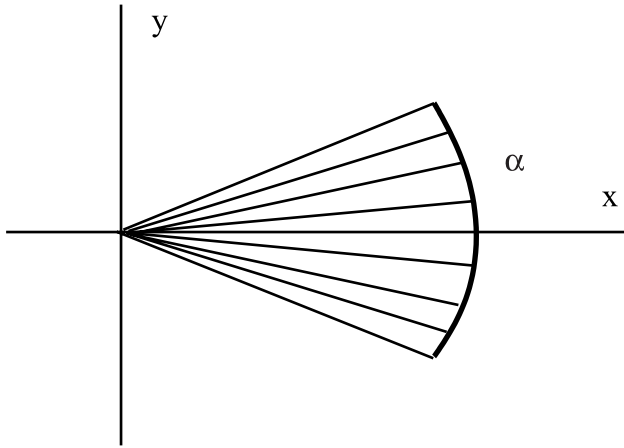


**Figure 14.** Schematic for assumed discharge geometry. The half-angle for the 2-dimensional fan shape is denoted by  $\alpha_0$ .

[47] The sequence of impulsive radiation prior to a negative ground stroke, and apparently associated with a normal lightning flash, shows some degree of polarization. These pulses would be classified as TIPP events if they were isolated in time and were VHF intense.

[48] Finally, we explore a little further the physical significance of the polarization. The VHF intense TIPP events, as presented in this study, tend to be isolated in time [Jacobson *et al.*, 1999], and appear to be associated with initial, virgin air breakdown. We are not certain in detail how the breakdown is formed and what exact process accounts for the TIPP VHF radiation. However, if we assume a TIPP is similar to the first corona discharge that initiates a sequence of negative discharge steps, the form of the TIPP discharge could be simulated as a composite of filaments that arranged in a cone-shaped geometry [Bacchiaga *et al.*, 1996]. If the satellite views the TIPP from the side of the cone, the cone will appear in projection as a two-dimensional fan. To simplify the discussion, we now assume a fan-shaped discharge with uniformly distributed filaments, as shown in Figure 14. We further assume that the amplitude of the radiation field is linearly related to the extent of the filaments, which in Figure 14 are all the same. Under these assumptions, the discharge will produce a linear polarization radiation along the  $x$  axis, with a certain degree of polarization. The degree of polarization can be estimated by the ratio of  $\langle E_x^2 \rangle / (\langle E_x^2 \rangle + \langle E_y^2 \rangle)$ , with  $\langle E_x^2 \rangle = \int E_0^2 \cos^2 \alpha \, d\alpha$  and  $\langle E_y^2 \rangle = \int E_0^2 \sin^2 \alpha \, d\alpha$ . If  $\alpha_0$  is the half-angle of the fan and is near to zero (or equivalently, for  $d$  near to 1),  $\alpha_0$  in radians can be approximated as,

$$\alpha_0 \sqrt{3(1-d)} \quad (3)$$

For the TIPP events displaying a degree of polarization 0.95, the half-angle  $\alpha_0$  is about  $22^\circ$ . This is a rather conservative estimate for  $\alpha_0$ , since the TIPP can be viewed from other angles rather than from broadside. At other viewing angles,  $\alpha_0$  will have to be smaller than  $22^\circ$  to be detected with the same degree of polarization. If the signal is completely unpolarized,  $\alpha_0$  is expected to equal  $90^\circ$ . The above equation will not work properly for large  $\alpha_0$  since it

was only an approximation for  $\alpha_0$  near to 0. For instance, for  $d = 0$ , the above equation gives  $\alpha_0 = 99^\circ$ , slightly greater than the expected value of  $90^\circ$ . With such a simple model, we can somewhat (in first order) relate the degree of polarization to the physical geometry of the discharge.

## 6. Conclusion

[49] For the selected VHF-intense TIPP events that occurred over the contiguous United States, we have found at least 40% are highly polarized, as compared to the concurrent background noise. Taking into account the effects of the magnetoionic mode splitting that frequently corrupts the coherence between the two modes, and therefore contaminates the detection of the polarization, we can further infer that most of the selected TIPPs are originally well polarized at their sources.

[50] The observations of the openness of the polarization ellipse  $\epsilon$  for the ordinary mode are in agreement with the predictions based on the FORTE antenna beam pattern and on the assumption that the mode has circular polarization as would be viewed in its propagation direction [Shao and Jacobson, 2001]. The fact that the two split modes appear as mirror images to each other in terms of the sense of polarization (Figure 2d) indicates that the original signals are linearly polarized. As expected, the original and the reflected pulses behave about the same in terms of the measured  $\epsilon$ .

[51] For the TIPPs that are detected with high degree of polarization and with relatively large ellipticity ( $|\epsilon| < 35^\circ$ ), the detected tilts of the ellipses  $\tau$  closely follow the predictions from the antenna-pattern model. Evidently, the tilt is in general orthogonal to the signal's arrival direction. As also expected, the tilts for a TIPP pair are determined to have about the same value. This, together with the  $\epsilon$  observations for the pulse pairs, indicates that both pulses in a TIPP arrive at the satellite from about the same nadir and azimuthal angles, consistent with the second pulse being a ground reflection of the first.

[52] Observations of a sequence of intermittent pulses, which appears to be associated with the early stage of a normal  $-CG$  flash, show that they are somewhat polarized, although not as highly polarized as the TIPP events. On the other hand, radiation produced by initial leader, dart leader and K streamer are detected with no recognizable polarization. For these "normal" lightning processes (in contrast to the TIPP events), the data was taken when the satellite was over the equatorial region so that the mode splitting is minimized. We also broaden the Fourier window to intentionally mix the two narrowly split modes and to increase the frequency resolution.

[53] Based on the polarization observations and the discussion of the associated physical significance, we inferred a possible breakdown mechanism for the TIPP events. If a TIPP is assumed to be a coherent discharge process that follows a cone-shaped geometry, the half-angle of the cone would be less than  $22^\circ$ . For radiation produced near the initial ground strokes, the composite of many simultaneous sources appear to be the reason for the random polarization. For dart leaders and K-streamers, which usually produce continuous VHF radiation at the propagating tip, the detected random polarization might be due to either the

tortuosity of the channel or the electric field environment near the propagating tip, or the both.

[54] We need to point out though that with the FORTE observations, the three-dimensional orientation of the polarization cannot be fully determined. The observations are two dimensional, and are only sensible to the wave plane normal to the propagation direction. Even in that plane, the effects of the Earth's ionosphere prevent a firm determination of the polarization orientation at the signal source.

[55] **Acknowledgments.** This work was performed at the Los Alamos National Laboratory under the auspices of the United States Department of Energy. We thank Daniel Holden and Charley Rhodes for helpful discussions on the performance of the FORTE antenna.

## References

- Bacchiega, G. L., A. Gazzani, M. Bernardi, I. Gallimberti, and A. Bondiou-Clergerie, Theoretical modeling of the laboratory negative stepped leader, paper presented at the 1994 International Aerospace and Ground Conference on Lightning and Static Electricity, Mannheim, Germany, May 24–27, 1996.
- Born, M., and E. Wolf, *Principles of Optics*, 5th ed., Pergamon, New York, 1975.
- Borovsky, J. E., An electrodynamic description of lightning return strokes and dart leaders: Guided wave propagation along conducting cylindrical channels, *J. Geophys. Res.*, *100*, 2697–2726, 1995.
- Budden, K. G., *The Propagation of Radio Waves*, Cambridge Univ. Press, New York, 1985.
- Cummins, K. L., M. J. Murphy, E. A. Bardo, W. L. Hiscox, R. Pyle, and A. E. Pifer, Combined TOA/MDF technology upgrade of U.S. National Lightning Detection Network, *J. Geophys. Res.*, *103*, 9035–9044, 1998.
- Davis, K., *Ionospheric Radio*, Peter Peregrinus, London, England, 1990.
- Holden, D. N., C. P. Munson, and J. C. Devenport, Satellite observations of transionospheric pulse pairs, *Geophys. Res. Lett.*, *22*, 889–892, 1995.
- Idone, V. P., Microscale tortuosity and its variations as observed in triggered lightning channels, *J. Geophys. Res.*, *100*, 22,943–22,956, 1995.
- Jacobson, A. R., S. O. Knox, R. Franz, and D. C. Enemark, FORTE observations of lightning radio-frequency signatures: Capabilities and basic results, *Radio Sci.*, *34*, 337–354, 1999.
- Jacobson, A. R., K. L. Commins, M. Carter, P. Klingner, D. Roussel-Dupre, and S. O. Knox, FORTE radio-frequency observations of lightning strokes detected by the National Lightning Detection Network, *J. Geophys. Res.*, *105*, 15,653, 2000.
- Kraus, J. D., *Radio Astronomy*, Cygnus-Quasar, Powell, Ohio, 1986.
- Massey, R. S., and D. N. Holden, Phenomenology of transionospheric pulse pairs, *Radio Sci.*, *30*, 1645–1659, 1995.
- Massey, R. S., D. N. Holden, and X. M. Shao, Phenomenology of transionospheric pulse pairs: Further observations, *Radio Sci.*, *33*, 1755–1761, 1998a.
- Massey, R. S., S. O. Knox, R. C. Franz, D. N. Holden, and C. T. Rhodes, Measurements of transionospheric radio propagation parameters using the FORTE satellite, *Radio Sci.*, *33*, 1739–1753, 1998b.
- Proctor, D. E., R. Uytendogaardt, and B. M. Meridith, VHF radio pictures of lightning flashes to ground, *J. Geophys. Res.*, *93*, 12,683–12,727, 1988.
- Rhodes, C. T., X. M. Shao, P. R. Krehbiel, R. J. Thomas, and C. O. Hayenga, Observations of lightning phenomena using radio interferometry, *J. Geophys. Res.*, *99*, 13,059–13,082, 1994.
- Shao, X. M., and A. R. Jacobson, Polarization observations of broadband VHF signals by the FORTE satellite, *Radio Sci.*, *36*, 1573–1589, 2001.
- Shao, X. M., and P. R. Krehbiel, The spatial and temporal development of intracloud lightning, *J. Geophys. Res.*, *101*, 26,641–26,668, 1996.
- Shao, X. M., P. R. Krehbiel, R. J. Thomas, and W. Rison, Radio interferometric observations of cloud-to-ground lightning phenomena in Florida, *J. Geophys. Res.*, *100*, 2749–2783, 1995.
- Shao, X. M., C. T. Rhodes, and D. N. Holden, RF radiation observations of positive cloud-to-ground flashes, *J. Geophys. Res.*, *104*, 9601–9608, 1999.
- Smith, D. A., X. M. Shao, D. N. Holden, C. T. Rhodes, M. Brook, P. R. Krehbiel, M. Stanley, W. Rison, and R. J. Thomas, Distinct, isolated thunderstorm radio emissions, *J. Geophys. Res.*, *104*, 4189–4212, 1998.
- Suszczynsky, D. M., M. W. Kirkland, A. R. Jacobson, R. C. Franz, S. O. Knox, J. L. L. Guillen, and J. L. Green, FORTE observations of simultaneous VHF and optical emissions from lightning: Basic phenomenology, *J. Geophys. Res.*, *105*, 2191–2201, 2000.
- Uman, M. A., *The Lightning Discharge*, Academic, San Diego, Calif., 1987.

---

A. R. Jacobson and X.-M. Shao, Space and Atmospheric Sciences Group NIS-1, MS D477, Los Alamos National Laboratory, Los Alamos, New Mexico 87545, USA. (xshao@lanl.gov)